Anomalous Pumped and Unpumped I-V Characteristics of Nb SIS Terahertz Mixers with NbTiN Striplines

B. Leone[†], B.D. Jackson[‡], J.R. Gao[§], T.M. Klapwijk[§],
W.M. Laauwen[‡] and G. de Lange[‡]

[†]University of Groningen,
Department of Applied Physics and Material Science Center,
Nijenborgh 4.13, 9747 AG Groningen, The Netherlands
[§]Delft University of Technology,
Department of Applied Physics and Delft Institute for Microelectronics
and Submicron Technology (DIMES)
Lorentzweg 1, 2628 CJ Delft, The Netherlands
[‡]Space Research Organization of the Netherlands,
Postbus 800, 9700 AV Groningen, The Netherlands

Abstract

To achieve nearly quantum limited noise temperatures around 1 THz in Nb SIS mixers NbTiN is used as stripline material because its high DC conductivity and gap frequency above 1 THz should minimize RF losses. However, one expects problems at the Nb/NbTiN interface due to an energy gap discontinuity. Indeed, the measured I-V curves show features that are absent in all Nb SIS mixers or Nb junctions with normal metal striplines. These include the gap voltage backbending and a severe gap voltage reduction in the pumped case. In an analysis of the unpumped case, it was previously shown that the backbending feature is caused by the DC heat trapped at the Nb/NbTiN interface and that the heat flow is limited by the electron-phonon interaction time. In the present paper, the analysis is extended to the pumped case by introducing an additional power contribution to explain the severe gap depression. This additional power results from the energy spectrum of the photon assisted tunneling electrons as given in the Tien-Gordon theory. Theoretical fits are obtained that faithfully reproduce the main features of the anomalous pumped I-V characteristcs.

1 Introduction

Until recent experimental results obtained at the Space Research Organization of the Netherlands (SRON) and Delft University of Technology, [1, 2] the lowest noise temperature around 1 THz was obtained using a Nb SIS mixer with Al tuning circuits. [3] However, a major limiting factor in the mixer performance is the loss in the aluminum striplines. [4] Therefore, one strategy to improve on these results is to use a superconducting stripline material with an energy gap

above the signal photon energy. NbTiN has been shown to be a good candidate both because of its frequency gap larger than 1 THz and its low RF loss. [5–12] However, because of the energy gap discontinuity at the Nb/NbTiN interface one expects problems with this structure. Understanding these is essential to evaluate the mixer performance.

2 ANOMALOUS I-V CHARACTERISTICS

The device structure of the Nb SIS mixers with NbTiN striplines investigated here is shown in Fig.1(a). The Nb junction is sandwiched between two NbTiN leads, which, in combination with an insulator SiO_2 layer, form a stripline that functions as an integrated tuning circuit for the mixer. The SIS device is a standard $Nb/Al–AlO_x/Nb$ junction with an area of typically 0.6 μm^2. Junctions with two critical current densities, 6.5 and 12 kA/cm^2, were used. The thickness of both Nb electrodes is 90 nm. The top and bottom NbTiN leads are 400 nm and 280 nm thick, respectively. The critical temperatures of Nb and NbTiN in the device were measured to be 9.1 K and 14.3 K. Device fabrication is described elsewhere. [11] The first I-V measurements on these devices were presented earlier [11] and are reproduced in Fig.2. These showed two striking features believed to be caused by the presence of the gap discontinuity. Firstly, a severe gap depression which worsens with increasing pumping level. Secondly, the gap depression can be seen within the same curve as a backbending of the gap voltage.

3 UNPUMPED CASE

The energy diagram of Fig.1(b) corresponds to the device structure for the two electrodes biased at the Nb gap voltage and shows the different energy gaps of Nb and NbTiN. The tunneling electrons see a potential barrier at the Nb/NbTiN interface. In a previous paper [13] we showed that in such a situation there is no quasiparticle trapping. Instead, the charges are Andreev reflected at the interface. As a result, charge is transported across the interface but the quasiparticle equilibrium temperature is raised in both electrodes. Here the assumption is made that the electron-electron interaction time is short enough to obtain a Fermi-like electron energy distribution in the junction. The BCS theory is used to determine the electron temperature from the backbending data, which yields the energy gap, Δ, through the following expression, [14]

$$\frac{1}{N(0)\beta} = \int_0^{\hbar\omega_c} \frac{\tanh\left[(2kT)^{-1}\sqrt{\epsilon^2 + \Delta^2}\right]}{\sqrt{\epsilon^2 + \Delta^2}} d\epsilon, \qquad (1)$$

where $N(0)$ is the density of states at the Fermi level, β is the BCS interaction constant and $\hbar\omega_c$ is the Debye frequency and is much greater than kT_c, where T_c is
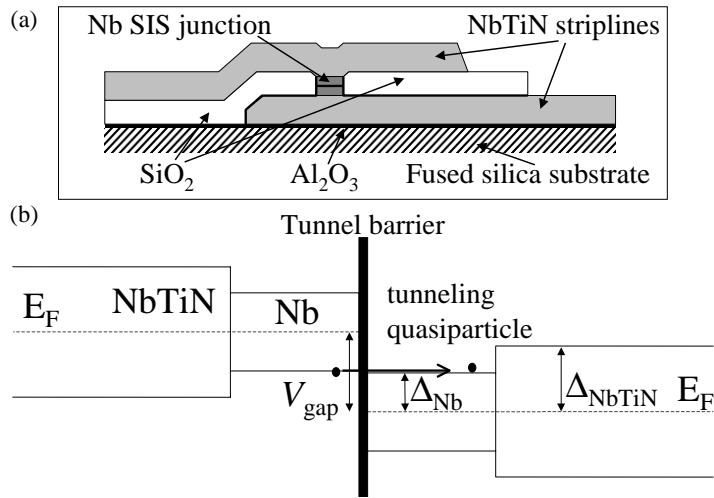
Figure 1: (a) Sketch of the cross-section of a Nb SIS junction with NbTiN striplines. (b) Energy diagram showing the relative energy gaps of Nb and NbTiN under the application of a bias voltage V_{gap} equal to the gap voltage of Nb.
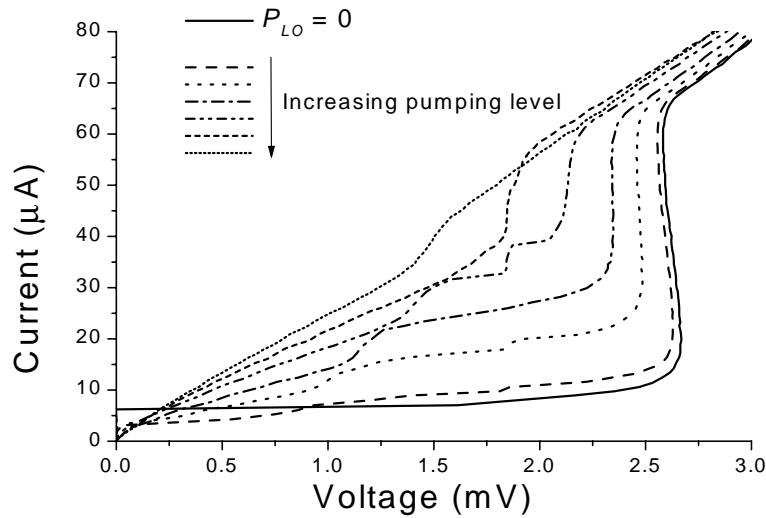

Figure 2: Anomalous pumped and unpumped I-V characteristics of a Nb/Al–AlO$_x$/Nb junction with NbTiN striplines at a local oscillator frequency of 895 GHz and a bath temperature of 4.7 K.

the critical temperature of Nb. It was further shown that the heat flow is governed by the electron-phonon interaction time which acts as the heat flow bottleneck of the system and the heat balance equation is given by

$$P_{DC} = \alpha_{heat}(T - T_b), \tag{2}$$

where P_{DC} is the DC power in the junction; T and T_b are the electron and bath temperatures, respectively. The heat transfer coefficient, α_{heat}, is given by

$$\alpha_{heat} = \frac{vC_e}{\tau_{eph}}, \tag{3}$$

where C_e is the electron heat capacity, τ_{eph} the electron-phonon interaction time and v the junction volume. Using the above, agreement with the DC I-V characteristics was demonstrated. In particular, quantitative agreement with the back-bending data was achieved.

4   PHOTON ASSISTED TUNNELING CONTRIBUTION

However, when the RF signal is coupled into the mixer the severe gap reduction shown in Fig.2 cannot be explained by Eq.2. Indeed, P_{DC} is only of the order of 100 nW, whereas the heating power required to produce the gap depression of, say, the dash-dotted pumped curve in Fig.2, ranges from 200 to 300 nW, depending on the accuracy of the heat transfer coefficient as obtained from the backbending data. Essentially, there are only two other power sources in our system that could possibly account for this additional required contribution. Firstly, the photon assisted tunneling (PAT) mechanism is responsible for the energy spectrum of the photon assisted tunneled electrons according to the Tien-Gordon picture. [15] In standard junctions, this added energy, delivered in multiples of the photon energy to the electron bath, escapes by heat diffusion. However, in the presence of heat trapping it will have to be dissipated within the electron bath, thus contributing to the overall junction heating. Secondly, because the mixer operates above the gap frequency of Nb, some RF dissipation in the junction is also expected. Let us first turn to the photon assisted tunneling mechanism. Tucker and Feldman [16] give an expression for the dissipative component of the local oscillator (LO) current, I'_{LO}, across the mixer

$$
\begin{aligned}
I'_{LO} &= \sum_{n=-\infty}^{\infty} J_n(\alpha)[J_{n-1}(\alpha) + J_{n+1}(\alpha)]I_{dc}(V + n\hbar\omega/e) \\
&= \sum_{n=-\infty}^{\infty} 2n\frac{J_n^2(\alpha)}{\alpha}I_{dc}(V + n\hbar\omega/e)
\end{aligned} \tag{4}
$$

where $J_n(\alpha)$ is the nth order Bessel function and its argument, $\alpha = eV_{LO}/\hbar\omega$, is the ratio of the energy associated with the LO voltage across the junction to the

photon energy; I_{dc} is the measured unpumped I-V characteristic and V is the bias voltage. We assume here that V_{LO} is a constant. Therefore, the photon assisted power, P_{PAT}, is the AC power associated with the dissipative current and is given by

$$
\begin{aligned}
P_{PAT} &= \frac{I'_{LO}V_{LO}}{2} \\
&= \sum_{n=-\infty}^{\infty} \frac{n\hbar\omega}{e} J_n^2(\alpha) I_{dc}(V + n\hbar\omega/e).
\end{aligned}
\tag{5}
$$

Intuitively, one can understand Eq.5 in the light of the Tien-Gordon theory [15] which pictures the pumped I-V characteristic as resulting from the sum from minus to plus infinity of the unpumped characteristic shifted by multiples of the photon energy and weighted by the corresponding Bessel function, i.e.

$$
I_{pumped} = \sum_{n=-\infty}^{\infty} J_n^2(\alpha) I_{dc}(V + n\hbar\omega/e).
\tag{6}
$$

One sees that Eq.5 multiplies the number of photon assisted tunneled quasiparticles by their corresponding energy, namely $n\hbar\omega$, for each value of n.

5 Theoretical fits to the anomalous pumped I-V curves

In order to produce theoretical fits of the pumped I-V characteristics, dedicated voltage-biased measurements were obtained, taking care to suppress the supercurrent and associated Shapiro steps, which are present in Fig.2. The pumped and unpumped experimental curves used for the theoretical calculations in this section are shown in Fig.4. The pumped measured data is used to calculate the DC power, P_{DC}, and is simply the product of the current by the voltage at each bias point. The photon assisted power, P_{PAT}, is calculated using Eq.5, where $I_{dc}(V)$ is the unpumped measured data. An appropriate value for the Bessel function argument, α, or, equivalently, V_{LO}, must also be chosen. However, since the actual LO power seen by the junction cannot be measured, V_{LO} must be treated as a fitting parameter. Its choice will be discussed later in this section. Fig.3 shows a plot of P_{DC}, P_{PAT} and their sum, $P_{Total} = P_{DC} + P_{PAT}$, as a function of bias voltage.

Using P_{Total} instead of P_{DC} in Eq.2 one can calculate a temperature profile as a function of bias voltage, $T(V)$, also shown in Fig.3. $T(V)$ is chosen to be constant upon reaching the critical temperature of Nb, which corresponds to the junction transition to the normal state. One can then calculate a unpumped theoretical I-V characteristic using the usual expression

$$
I_{dc} = \frac{-1}{eR_n} \int_{n=-\infty}^{\infty} N(E)N(E - eV)[f(E) - f(E - eV)]dE,
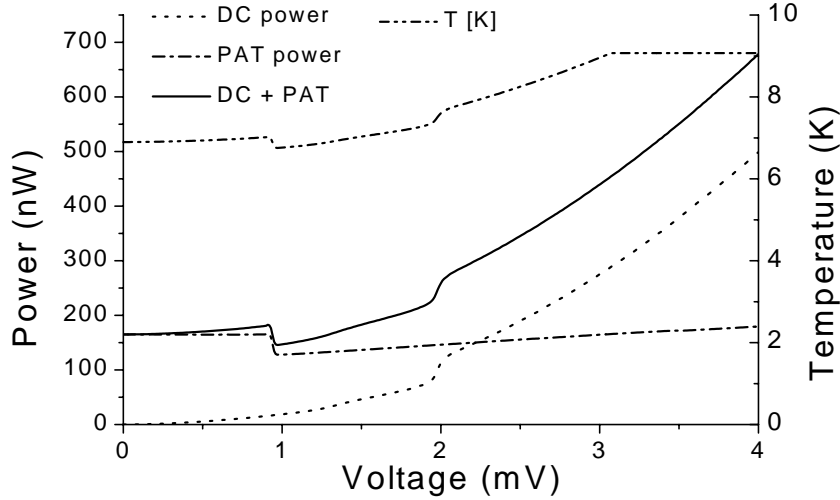\tag{7}
$$

Figure 3: DC, PAT and total=DC+PAT heating powers (nW), and junction temperature (K) corresponding to the DC+PAT case, versus bias voltage (mV).

where R_n is the normal state resistance, and taking care to assign to the density of states, $N(E) = N(E,T)$, and the Fermi-Dirac distribution function, $f(E) = f(E,T)$ the temperature profile $T(V)$. Fig.4 shows the I-V characteristic so obtained and labeled $I(V,T(V))$.

It should be appreciated that the calculated unpumped curve, $I(V,T(V))$, has the same gap voltage as the pumped data, unlike the measured unpumped curve. Furthermore, by inserting this theoretical curve into Eq.6 one obtains the curve labeled "Tien-Gordon" in Fig.4. This latter procedure is used to fit the LO voltage across the junction, V_{LO}. The fact that both the reduced gap and the photon step level are reproduced in the fit using only V_{LO} as fitting parameter, points to the self-consistency of our physical picture of the gap depression mechanism. However, as it stands, the calculated I-V characteristic fails to reproduce the correct photon step onset. This is due to the fact that, according to Eq.6, the photon onset reflects the gap voltage value shifted by a multiple of the photon energy. In fact, in our anomalous case, one should be careful that the value of the gap changes with the bias voltage according to the temperature profile. Hence, Eq.6 should be adjusted as follows,

$$I_{pumped} = \sum_{n=-\infty}^{\infty} J_n^2(\alpha) I_{dc}(V + n\hbar\omega/e, T(V)), \qquad (8)$$

where $I_{dc}(V + n\hbar\omega/e, T(V))$ is now calculated and given by Eq.7, the density of states and the Fermi-Dirac distribution functions shifted by multiples of the
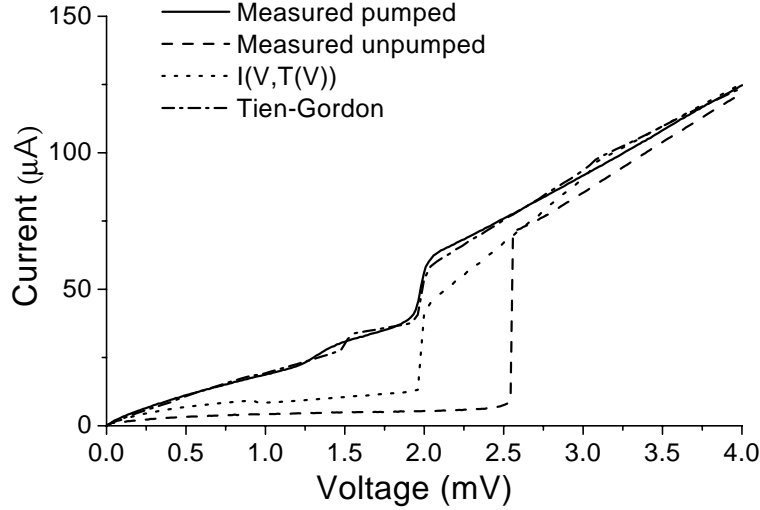
Figure 4: Pumped and unpumped data for a Nb/Al–AlO$_x$/Nb junction with NbTiN striplines at a local oscillator frequency of 845 GHz and a bath temperature of 5.7 K; the calculated unpumped I-V curves using the temperature profiles due to the total power, the DC power only and the PAT power only. The calculated pumped I-V curve using the total power temperature profile plugged into Eq.6 is also plotted.

photon energy are also a function of the temperature profile $T(V)$, for all values of n, and are given by $N(E + e(V + n\hbar\omega), T(V))$ and $f(E + e(V + n\hbar\omega), T(V))$, respectively.

Fig.5 shows the resulting fits to pumped data for two different pumping levels. Again, V_{LO} is the only fitting parameter and it can be seen that several anomalous pumped data features are reproduced. These are the gap depression, the photon step level, the photon step onset and the subgap current below the photon step onset. Deviations from the data are also present. Firstly, there is the smoothing of the measured photon step, which is usually ascribed to quasiparticle lifetime effects. Hence, if no smoothing functions are applied, the theoretical counterparts are generally characterized by much sharper gap and photon step onsets. [17] Secondly, the excess current in the measured data just above the gap could be explained by the fact that actual junctions are not, strictly speaking, SIS structures, on which the calculations are based, but more closely resemble SNIS structures, where N stands for the thin Al layer. Hence, the corresponding density of states will be modified accordingly. Thirdly, the calculated curves show an abrupt transition to the normal state around 3.1 mV, not present in the data. Here, the assumption of a constant heat transfer coefficient used for the fits, via Eq.2, breaks down. In fact, Eq.3 clearly indicates that α_{heat} should
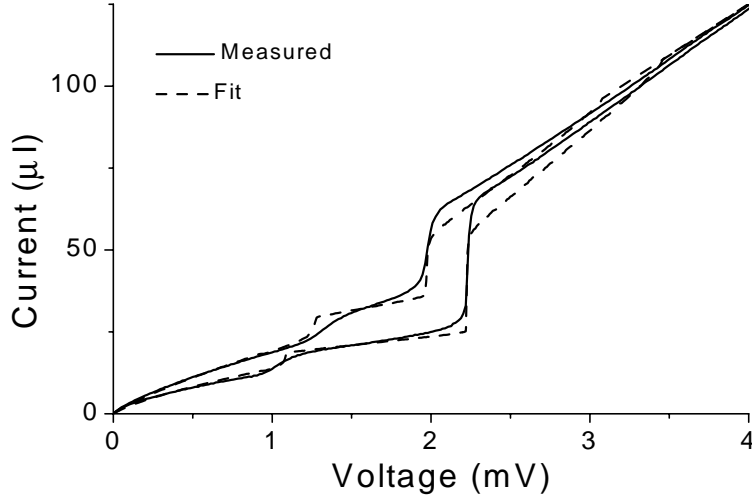
Figure 5: Pumped data of a Nb/Al–AlO$_x$/Nb junction with NbTiN striplines at a local oscillator frequency of 845 GHz and a bath temperature of 5.7 K for two different pumping levels fitted using Eq.8.

be temperature-dependent, however, since the temperature-dependent behavior of the electron-phonon interaction is rather complex and strongly dependent on material parameters, [18] it has been left out of this analysis. Suffice it to say that α_{heat} seems to vary very slowly with temperature across the bias voltage range of interest only to deviate significantly near the critical temperature. There are, nevertheless, indications that an abrupt transition to the normal state has been observed albeit at a higher bias voltage. [19]

Through the above exercise, it has been shown that the DC and PAT heating power contributions can reasonably explain the experimental data. This suggests that the possible contribution from RF absorption is negligible. Taking into account the fit resolution as well as the measurement error in the heat transfer coefficient, it can be estimated that the RF absorption in the junction, if present, should be less than 10% of the photon assisted tunneling contribution.

6 CONCLUSION

In conclusion, the heat trapping mechanism and the electron-phonon interaction-limited heat flow process responsible for the gap voltage backbending in the unpumped case are shown to be also responsible for the severe gap depression in the pumped case, provided one takes account of the additional heating power introduced by the photon assisted tunneling process. As a consequence, the proposed

solution [13] to reduce heating by increasing the Nb volume, while keeping the junction area unchanged, is also applicable in the RF case. Furthermore, in addition to explaining the backbending and gap depression anomalies quantitatively, the anomalous pumped I-V curves are also satisfactorily described theoretically.

REFERENCES

[1] B.D. Jackson, G. de Lange, W.M. Laauwen, J.R. Gao, N.N. Iosad, and T.M. Klapwijk. NbTiN and NbTiN/Al tuning circuits for thz SIS mixer. Published in these proceedings.

[2] A. M. Baryshev, B. D. Jackson, G. de Lange W. Laauwen, S. V. Shitov, J. R. Gao, and T. M. Klapwijk. Quasi-optical terahertz SIS mixer. Published in these proceedings.

[3] M. Bin, M.C. Gaidis, J. Zmuidzinas, T.G. Phillips, and H.G. LeDuc. Low–noise 1 THz niobium superconducting tunnel junction mixer with a normal metal tuning circuit. *Appl. Phys. Lett.*, 68:1714–1716, 1996.

[4] P. Dieleman, T.M. Klapwijk, J.R. Gao, and H. van de Stadt. Analysis of Nb superconductor–insulator–superconductor tunnel junctions with Al striplines for thz radiation detection. *IEEE Trans. on Appl. Supercond.*, 7:2566–2569, 1997.

[5] R. di Leo, A. Nigro, G. Nobile, and R. Vaglio. Niobium-titanium nitride thin films for superconducting rf accelerator cavities. *J. Low Temp. Phys.*, 78:41, 1990.

[6] J. W. Kooi, J. A. Stern, G. Chattodpadhyay, H. G. LeDuc, B. Bumble, and J. Zmuidzinas. Low–loss NbTiN films for THz SIS mixer tuning circuits. In R. Blundell and E. Tong, editors, *The Eighth International Symposium on Space Terahertz Technology: Symposium Proceedings*, pages 310–318, Harvard–Smithsonian Center for Astrophysics, Cambridge, MA, 1997.

[7] J. A. Stern, B. Bumble, H. G. LeDuc, J. W. Kooi, and J. Zmuidzinas. Fabrication and DC characterization of NbTiN based SIS mixers for use between 600 and 1200 GHz. In *Ninth International Symposium on Space Terahertz Technology: Symposium Proceedings*, pages 305–313, Jet Propulsion Laboratory, Pasadena, CA, March 1998.

[8] J. W. Kooi, J. A. Stern, G. Chattodpadhyay, H. G. LeDuc, B. Bumble, and J. Zmuidzinas. Low–loss NbTiN films for THz SIS mixer tuning circuits. *Intl. J. Infrared and MM Waves*, 19:373–383, 1998.

[9] J. Zmuidzinas, J. W. Kooi, J. Kawamura, G. Chattodpadhyay, J. A. Stern, B. Bumble, and H. G. LeDuc. Development of SIS mixers for 1 THz. *Proc. SPIE*, 3357:53–61, May 1998.

[10] J. Kawamura, D. Miller, J. Chen, J. Kooi, J. Zmuidzinas, B. Bumble, H.G. LeDuc, and J.A. Stern. Fabrication and DC characterization of NbTiN based SIS mixers for use between 600 and 1200 GHz. In *Proceedings of the Tenth International Symposium on Space Terahertz Technology*, page 398, University of Virginia, March 1999.

[11] B.D. Jackson, N.N. Iosad, B. Leone, J.R. Gao, T.M. Klapwijk, W.M. Laauwen, G. de Lange, and H. van de Stadt. Dc and terahertz response in nb sis mixers with nbtin striplines. In *Proceedings of the Tenth International Symposium on Space Terahertz Technology*, pages 144–156, University of Virginia, March 1999.

[12] N.N. Iosad, B.D. Jackson, T.M. Klapwijk, S.N. Polyakov, P.N. Dmitriev, and J.R. Gao. Optimization of rf- and dc-sputtered nbtin films for integration with nb-based sis junctions. *IEEE Trans. on Appl. Supercond.*, 9:1716–1719, 1999.

[13] B. Leone, B.D. Jackson, J.R. Gao, and T.M. Klapwijk. Geometric heat trapping in niobium superconductor–insulator–superconductor mixers due to niobium titanium nitride leads. *Appl. Phys. Lett.*, 76:780–782, 2000.

[14] M. Tinkham. *Introduction to Superconductivity*. McGraw-Hill, New York, 2nd edition, 1996. p. 63.

[15] P.K. Tien and J.P. Gordon. Multiphoton process observed in the interaction of microwave fields with the tunneling between superconductor films. *Phys. Rev.*, 129:647–651, 1963.

[16] J.R. Tucker and M.J. Feldman. Quantum detection at millimeter wavelengths. *Rev. of Mod. Phys.*, 57:1055–1113, 1985.

[17] L. Solymar. *Superconductive Tunnelling and Applications*. Chapman and Hall, London, 1972. p. 43.

[18] E.M. Gershenzon, M.E. Gershenzon, G.N. Gol'tsman, A.M. Lyul'kin, A.D. Semenov, and A.V. Sergeev. Electron-phonon interaction in ultrathin nb films. *Sov. Phys. JETP*, 70:505–511, 1990.

[19] Unpublished results.